Journal of Medical and Biological Engineering (2018) 38:735–743
https://doi.org/10.1007/s40846-017-0345-y

ORIGINAL ARTICLE

Multienzymatic Cholesterol Nanobiosensor Using Core–Shell Nanoparticles Incorporated Silica Nanocomposite

Rajshri K. Satvekar[1] · **Shivaji H. Pawar**[2]

Received: 28 December 2016 / Accepted: 19 September 2017 / Published online: 3 January 2018

Abstract

The silica sol–gel matrix was prepared with tetraethyl orthosilicate as a precursor by sol–gel method besides functionalized with bovine serum albumin to minimize cracking and to stabilize enzymes for biosensing. Core–shell Fe_3O_4@C@Ag NPs are prepared using a facile method and applied to enhance electron transfer between enzymes and electrode surface. The Fe_3O_4 NPs prepared by modifying co-precipitation method; subsequently depositing carbon and silver on Fe_3O_4 NPs core by the facile green approach. Fe_3O_4@C@Ag NPs and silica/Fe_3O_4@C@Ag nanocomposite have been characterized by Fourier Transform Infra-Red spectroscopy, UV–visible spectroscopy, and X-ray diffraction technique. The surface topographies of the nanomaterials were investigated by Scanning electron microscopy and Transmission electron microscopy. Cyclic voltammetry employed to study the electrochemical behavior of nanobiosensor. The sensitivity of modified electrode is 0.0346 $\mu AmM^{-1}cm^{-1}$ with detection limit 0.5 mM. The high sensitivity of the biosensor is attributed to the large surface area of Fe_3O_4@C@Ag NPs for effective loading of HRP besides its high electron communication capability with the aid of enhanced selectivity and anti-interference ability due to the silica sol–gel matrix immobilized with ChOx.

Keywords Silica nanocomposite · Cholesterol nanobiosensor · Immobilization · Core–shell nanoparticles · Sol–gel matrix · Horseradish peroxidase · Cholesterol oxidase

1 Introduction

Biosensors are widely used in medical diagnosis to detect the biomarker of various diseases and disorders starting from diabetes to cancer. Nanobiosensor offers the potential to fulfill these criteria through an interdisciplinary combination of approaches from nanotechnology, chemistry, and medical sciences. A specific biomarker indicates a healthy or diseased state. Among the various diseases, three of them are important because of their worldwide incidence, prevalence, morbidity and mortality; namely diabetes, cardiovascular diseases (CVD), and cancer. CVD diseases are highly preventable, yet these are a major cause of death in humans over the world. Recent years, the demand has been grown in the field of medical diagnosis for a sensitive, reliable, and cost-effective biosensor which can consent rapid detection of cholesterol.

Cholesterol is an essential building block in the structure of cells, used in making hormones and vitamin D, and for producing energy. Two major types of cholesterol are found in the blood: low-density lipoproteins (LDL), the harmful substance and high-density lipoproteins(HDL), the protective substance. Maintaining the accurate balance of each is essential to help reduce the risk of heart attacks and stroke linked with high cholesterol. High total cholesterol level (the sum of free cholesterol and cholesterol esters) can cause damage of blood vessel resulting in coronary heart disease and peripheral vascular disease. The preferred total plasma cholesterol for an individual is less than 5.2 mM (200 mg dL^{-1}), while a high level considered as greater than 6.2 mM (240 mg dL^{-1}) [1].

An elevated level of cholesterol is associated with many diseases and disorders such as arteriosclerosis, cerebral

Electronic supplementary material The online version of this article (https://doi.org/10.1007/s40846-017-0345-y) contains supplementary material, which is available to authorized users.

✉ Rajshri K. Satvekar
rajshrinaik5@gmail.com

[1] Center for Interdisciplinary Research, D.Y. Patil University, Kolhapur 416006, MS, India

[2] Director of Centre for Research and Technology Developments, Sinhgad Institutes, Solapur 413256, MS, India

thrombosis, hypothyroidism, hypertension, and myocardial infarction. Accordingly, an urgent need to fabricate reliable and sensitive total cholesterol biosensor for detection of cholesterol in clinical samples is essential [2]. Conferring to 2011 figures from the World Health Organization (WHO), cardiovascular diseases is the world's biggest killers, claiming more than 17 million lives each year worldwide. Cholesterol levels are generally monitored via diagnostic testing, but the optimal monitoring interval is unknown and practice varies. However, it is still highly desirable and technologically important to synthesize nanocomposite with a well-defined shape structure for cholesterol nanobiosensing.

Electrochemical cholesterol nanobiosensors offer several advantages such as the small size, inexpensive, minimum volume and power requirements for analysis; having great promise for a wide range of biomedical and environmental applications. The cholesterol nanobiosensor sensitivity is predominantly governed by the ability of immobilized enzymes to exchange electrons with maximum electron transfer rate. High porosity and surface area of silica matrices allow encapsulation of higher amount of the enzymes without reducing their biofunctionality and accessibility. Nevertheless, functionalization of silica sol–gel matrices by conducting nanomaterials is essential for direct electrochemistry of cholesterol enzymes [3].

Bovine serum albumin (BSA) is a renowned inert protein with 35 reactive primary amino groups which provide thermo-stabilization of several enzymes [4]. This is likely due to the preservation of enzyme structure by BSA. The mechanism of stabilization has been linked to hydrophobic interactions. When immobilized in a redox polymer, BSA has been shown to stabilize the electrochemical response of the polymer due to the prevention from over-swelling. Consequently, in this work BSA is utilized to prevent cracking and to stabilize immobilized enzymes for biosensing.

In recent times, core–shell nanoparticles are promising nanomaterial for the biomedical applications in many arenas owing to its multifunctional properties, which can be tailored by changing the core to shell ratio of constituting materials. The carbon and silver coated magnetic nanoparticles are one of the most attractive core–shell nanoparticles for its chemical activity, and biocompatibility for biomedical applications [5–7]. Fe_3O_4 nanoparticle (NP) is favorable material in due to its numerous properties utilized in abiomedical application. They have already gained substantial attention in immobilization of biomolecules such as enzymes, antibodies, and anticancer agents [8–10]. However, there are few limitations in the application of Fe_3O_4 NPs as they are prone to aggregation in aqueous solution. Hence, acoating of the Fe_3O_4 NPs is essential with other materials protects them from being aggregated to immensely widen their application.

Carbon is a frequently used as a matrix, owing to its good ionic conductivity, and low volume expansion. Various methods are used to synthesize composites of nanomaterials embedded in carbon matrices, including hydrothermal/solvothermal reaction, electro-spinning, and chemical deposition [11]. Recently, a new carbon material which is prepared by glucose has aroused much concern [12]. The current research on the green processing of carbon nanomaterials is progress on: (i) energy-efficient and less-toxic chemical modification using covalent-bonding functionality, and (ii) non-covalent bonding methods like physical modification using green solvents and dispersants [13]. Thus, in this work glucose is utilized as a carbon source for carbonaceous coating and simultaneously acts as areducing agent for silver coating. The preparation process belongs to "green chemistry" as the reaction process is safe and does not acquire any contamination of the environment [14].

As compared to other shells, carbonaceous shells have higher stability in acidic or basic media, along with high temperatures and pressures. Furthermore, the outer polysaccharide shell has various functional groups such as carboxylic, aldehyde, and hydroxyl groups [15]. These shells are highly porous and have a large surface area which is beneficial for various biomedical applications. Moreover, silver shell aids the conductivity for nanobiosensorapplication. Number of cholesterolnanobiosensors [16–19] has been described over the past 30 years.Cholesterol enzymatically determined by various methods such as fiber-optic fluorescence and luminescence, fluorometric, spectrophotometric, and potentiometric biosensors.These methods suffer from interference fromother substances found in the blood such as ascorbic acid and uric acid. Therefore, electrochemical cholesterol nanobiosensoris designed based on silica sol–gel matrix incorporated with Fe_3O_4@C@Ag NPs to determine the total cholesterol level.

In this work, silica sol–gel matrix was integrated with Fe_3O_4@C@Ag NPs and employed to immobilize ChOx, ChEt, and HRP. A facile and efficient method have been utilized for the synthesis of core–shell nanoparticles comprising the core of Fe_3O_4 NP with inner amorphous carbon shell and outer metallic Ag shell as illustrated in Fig. 1. The prepared core–shell nanoparticles dispersed in silica sol to form silica nanocomposite which is becoming an interesting platform for the development of cholesterol nanobiosensor.

2 Experimental

2.1 Materials and Method

Cholesterol Oxidase (ChOx, EC 1.1.3.6, C-8649, 18 U/mg), cholesterol esterase (ChEt, EC 3.1.1.13, 200 U/mg), HRP (EC 1.11.1.7, 150 U/mg), tetraethyl orthosilicate (TEOS), Triton X, cholesterol oleate, cholesterol, glucose, and ITO coated glass plates (1.1 mm thickness, resistivity 70–100

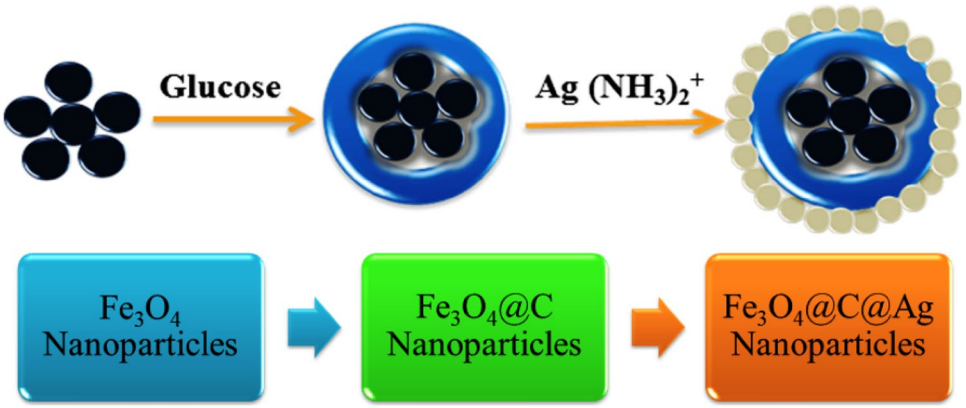

Fig. 1 Schematic diagram of the stepwise growth mechanism of carbonaceous and silver shell on Fe_3O_4 NPs

Ω) were procured from Sigma-Aldrich. Hydrogen peroxide (30 w/v % solution), silver nitrate ($AgNO_3$), ferrous sulfate heptahydrate ($FeSO_4{\cdot}7H_2O$) and ferric chloride hexahydrate ($FeCl_3{\cdot}6H_2O$) were purchased from Hi Media, India. All other reagents were of analytical grade obtained from SD Fine Chemical Pvt. Ltd. India and used without further purification. All solutions were prepared with deionized double distilled water.

Silica/Fe_3O_4@C@Ag nanocomposite was characterized by scanning electron microscopy (SEM) (JEOL JSM-6360 LA) equipped X-ray Microanalysis system, UV–visible spectroscopy (UV-2550, Shimadzu Co., Japan), Fourier transform infrared spectroscopy (FTIR) (Nicolet 510 P) and X-ray Diffraction (XRD) (Rigaku Miniplex). Transmission electron microscopy (TEM) images were achieved with a Hitachi Model H-800 (Hitachi, Japan) opened at an accelerating voltage of 100 kV. For TEM measurements, Silica/Fe_3O_4@C@Ag nanocomposite suspension was dispensed onto a copper grid covered with a continuous carbon film. Cyclic voltammetry (CV) was executed by using a CHI660C electrochemical workstation (CH Instruments, Shanghai, China). A three-electrode system was used, comprising a working ChOx/ChEt/HRP/Silica/Fe_3O_4@C@Ag nanocomposite modified ITO electrode, an Ag/AgCl reference electrode and a platinum wire counter electrode. All experiments were carried out at room temperature (25 ± 2 °C).

2.2 Synthesis of Magnetic Nanoparticles

Fe_3O_4 NPs have been prepared by chemical co-precipitation method under alkaline conditions using sodium hydroxide (NaOH) as the base [6]. Briefly, the molar ratio of Fe^{2+}/Fe^{3+} was fixed at 1.0 to produce MNPs with an average particle size of 7.0 nm. Iron (III) chloride hexahydrate ($FeCl_3{\cdot}6H_2O$, 0.1 M) and iron (II) sulfate heptahydrate ($FeSO_4{\cdot}7H_2O$, 0.1 M) were mixed in strongly stirred NaOH (3.0 M) solution in de-ionized water at 88 °C for 15 min. The black precipitate product was magnetically decanted, washed with ethanol and water to remove cations and anions. The Fe_3O_4 NPs were dried at 50 °C for 6 h in a vacuum oven.

A homogeneous Fe_3O_4 NPs suspension was prepared by dispersing 1.0 mg Fe_3O_4 NPs into 10.0 mL doubly distilled water by 1 h ultrasonic agitation. Subsequently, glucose (0.5 g mL^{-1}) was mixed in Fe_3O_4 NPs suspension and stirred for 0.5 h to properly adsorbed on the Fe_3O_4 NP surfaces; abbreviated as solution-I. The solution-II was prepared by slowly adding ammonia solution (25 %) in anaqueous solution of $AgNO_3$ (0.06 M) to form Ag $(NH_3)_2^+$ solution. Then, solution-II was stirred for sufficient adsorption of Ag $(NH_3)_2^+$ on Fe_3O_4@C nanospheres were glucose was acting as reducing agent. Final solution was heated in a water bath at 50 °C for 30 min. Magnetic decantation of the slightly brown product was carried out by using magnets. The flask containing nanoparticle is put in the vicinity to the magnet to separate impurities and repeatedly washed with water. Afterwards, nanoparticles dispersed in ethanol and dried at 60 °C for 6 h in a vacuum oven.

2.3 Preparation of Silica/Fe_3O_4@C@Ag Nanocomposite

Silica sol was prepared by the hydrolysis and polycondensation of tetraethyl orthosilicate as a precursor which is described in the previous report [20]. Then the appropriate amount of BSA was added to the solution, under constant stirring to functionalize silica sol. After 24 h aging, Fe_3O_4@C@Ag NPs were dispersed in the silica sol by stirring at room temperature. Afterward, it was sonicated for 1 h to obtain viscous silica sol with highly dispersed Fe_3O_4@C@Ag NPs to synthesize silica/Fe_3O_4@C@Ag nanocomposite of pH 7.4 were prepared. These enzyme solutions added in the silica/Fe_3O_4@C@Ag nanocomposite solution for encapsulation of enzymes.

2.4 Fabrication of Cholesterol Nanobiosensor

Indium Tin Oxide (ITO) glass plates were sonicated with acetone and ethanol solution; then washed with distilled water and dried at room temperature. ChOx (1.0 mg mL^{-1}) and HRP solution (2.0 mg mL^{-1}) in potassium phosphate buffer of pH 7.0 and ChEt (2.0 mg mL^{-1}) in potassium phosphate buffer solution were spin coated onto a 1.0 cm^2 area of ITO electrode surface and kept at 4 °C for 12 h in a humid chamber.

3 Results and Discussion

3.1 Formation Mechanism of the Silica/Fe_3O_4@C@Ag Nanocomposite

Eco-friendly glucose as a carbon source is utilized for carbonaceous coatings on Fe_3O_4 NPs. Additionally, glucose is used as a mild reducing agent, which deals with the tailored shell growth of silver onto Fe_3O_4 NPs. These two facets of glucose ensure the coating of carbon and synchronized reduction of Ag^+ ions adsorbed onto Fe_3O_4 NPs; fabricating the core–shell Fe_3O_4@C@Ag NPs. The added Ag^+ ions are reduced to a metallic state and subsequently bound the Fe_3O_4 NPs results in transparent supernatant liquid. The dry black mass of Fe_3O_4 NPs after carbon and silver coating turned to glittery brownish. The structure and composition of the core–shell nanoparticles and silica nanocomposites were further characterized by XRD, UV–Visible, FTIR, SEM, and TEM.

3.2 X-ray Diffraction (XRD)

XRD patterns of silica (a), silica/Fe_3O_4@C@Ag nanocomposite (b), and Fe_3O_4@C@Ag NPs (c) were illustrated in Fig. 2. XRD pattern of silica (a) displays a peak of low intensity and expressive width indicating amorphous structure, with a halo centered peak on 23°. As compared to the standard XRD pattern of Fe_3O_4 NPs (JCPDS Card no. 79-0419, magnetite) and Ag (JCPDS Card no. 89-3722, face centered); the XRD pattern of Fe_3O_4@C@Ag NPs (c) displays diffraction peak at 35.560°, 38.098°, 44.419°, 62.970°, 64.540°, and, 77.362° which are assigned to the (311), (111), (200), (440), (220), and, (311). The results indicate that Fe_3O_4@C@Ag NPs composed of crystalline Fe_3O_4 and Ag; while carbon coating is amorphous in nature. The broad reflection peaks were owed to the particle size of nanodomain. The diffraction of silica/Fe_3O_4@C@Ag nanocomposite (b) visibly indicates interaction of silica sol–gel matrix with Fe_3O_4@C@Ag NPs with the hump at 23–24°. The decrease in the crystallinity may be due to the introduction of bulky silica polymeric chain, which validates that the

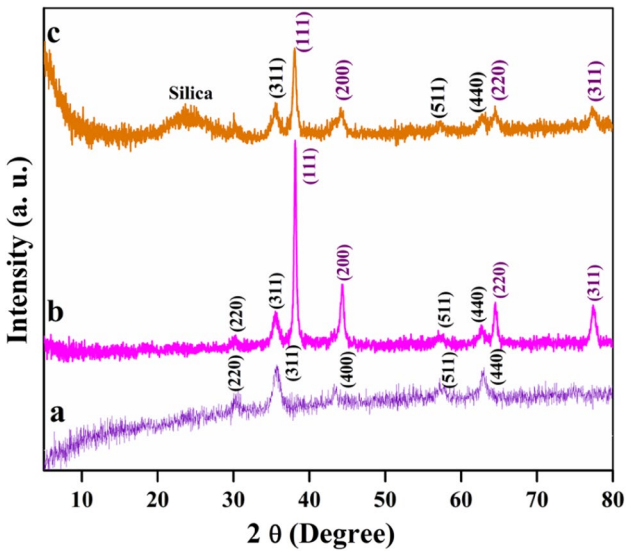

Fig. 2 X-ray diffraction pattern of **a** Fe_3O_4 Nps, **b** Fe_3O_4@C@Ag NPs, and **c** Silica/Fe_3O_4@C@Ag nanocomposite

integration of silica suppressed the crystallization to some degree.

3.3 Structural Morphology

The morphology and structure of the synthesized Fe_3O_4@C@Ag NPs were observed using transmission electron microscopy (Fig. 3a); showing that the Fe_3O_4@C@Ag NPs were very fine and spherical shape. It displayed carbonaceous coating (~ 2–3 nm) on Fe_3O_4 nanoparticles to form C@Fe_3O_4 nanospheres (~ 80 nm). In addition, these are wrapped by small spherical Ag nanoparticles (~ 16.96 nm). An average particle size of core–shell Fe_3O_4@C@Ag NPs from TEM image is estimated to be 100.0 ± 2 nm.

The selected area electronic diffraction (SAED) patterns shown in Fig. 3a Inset; display spotty diffraction rings attributed to crystalline feature. A high-resolution TEM image is displayed in Fig. 3b documented for single Fe_3O_4@C@Ag NPs, clearly demonstrating the Fe_3O_4 NPs were enveloped with carbon moieties and Ag nanoparticles developed around the Fe_3O_4@C nanospheres with lattice fringes.The contrast of a carbon layer was strong as compared to the Ag shell, may be due to the concentration of glucose utilized.

According to SEM image (Fig. 4a), sphere shaped Fe_3O_4@C@Ag NPs shows a uniform distribution of sphere clusters of average size ~ 100 nm. SEM image of Silica/Fe_3O_4@C@Ag nanocomposite (b) shows smooth surface and uniform structure; ascertaining the silica sol–gel matrix and Fe_3O_4@C@Ag NPs incorporated homogeneously [Fig. S1] with a good compatibility devoid of phase separation. The EDS spectra of Fe_3O_4@C@Ag NPs and Silica/Fe_3O_4@C@Ag nanocomposite also confirm the presence of

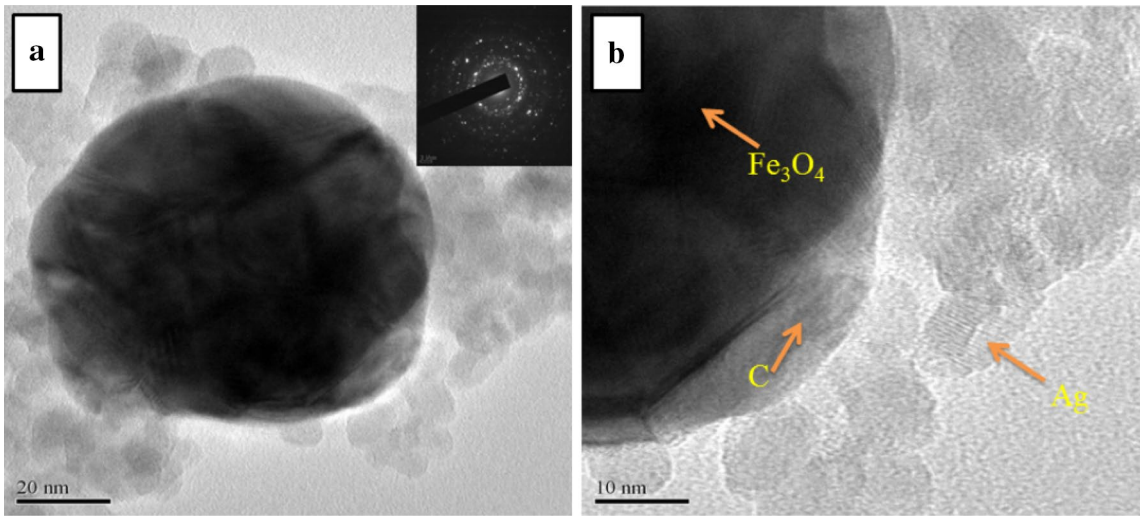

Fig. 3 TEM image of **a** Fe_3O_4@C@Ag NP (Inset: SAED pattern) and **b** High-resolution TEM of Fe_3O_4@C@Ag NP

C, O, Si, Ag and Fe and quantitative elemental composition listed in the respective figure.

Furthermore, elemental X-ray Microanalysis was conducted for confirmation of successful dispersion of reinforcement material in silica nanocomposite. The electron beam penetrates 2–3 microns beneath surface of the thin film to expose embedded silica, silver, and iron distribution. X-ray mapping analysis of silica/Fe_3O_4@C@Ag nanocomposite represents the bright spots signifying that silica and iron element clearly illustrates a homogenous distribution (Fig. 4e).

3.4 Spectroscopic Analysis

Figure 5b displayed the strong characteristic peak appeared at 420 nm in UV–Visible absorption spectra, which is assigned to Fe_3O_4@C@Ag NPs. According to Mie's theory, the single SPR band is expected in absorption spectra of spherical metal nanoparticles, although anisotropic particles could give rise to two or more SPR bands depending on the shape of particles. Herein, a single SPR band is observed specifies that nanoparticles are spherical in shape and equivalent with the TEM observations.

FTIR was employed for the conformational study of enzymes to investigate the characteristic structures of enzymes after entrapment in silica/Fe_3O_4@C@Ag nanocomposite. FTIR spectra of a pure solution of enzymes (a) in potassium phosphate buffer of pH 7.0 and ChOx, ChEt and HRP entrapped in silica/Fe_3O_4@C@Ag nanocomposite is shown in Fig. 6b. It specifies amide I (C=O) stretch at 1641 cm^{-1}, and amide II (N–H) at 1535 cm^{-1}. After immobilization in nanocomposite it shows a reduction in intensity at N–H regions; illustrates the hydrogen bonding of an amine group with Si–O of silica.

3.5 Optimization

A well-defined cyclic voltammograms and good response to cholesterol oleate were observed in the 0.1 M potassium phosphate buffer solution containing 0.1 M KCl. The effect of buffer pH on the response for cholesterol oleate was investigated and the results showed that the optimum pH range of phosphate buffer was 6.8 to 7.3. In general, Triton X-100 a non-ionic surfactant is contained in the sample solution for solubilizing cholesterol since cholesterol is a sparingly soluble substance in aqueous solution. Triton X-100 also plays an important role in stabilizing the activity of cholesterol oxidase. However, at high concentrations, it inhibits the activity of cholesterol oxidase [21]. Especially, when the cholesterol oxidase electrode is repeated used, a decrease in response current is observed. The effect of Triton X-100 concentration on peak current was examined and an optimum concentration range was found in 0.7–1.2% (V/V). The phosphate buffer (pH 7.0) with 0.1 mol L^{-1} KCl and 0.8% Triton X-100 was chosen for further experiments.

3.6 Electrochemical Analysis

Cyclic voltammograms (Fig. 7) were recorded within potential range of 0.65–0.15 V with a scan rate of 0.1 Vs^{-1} in a 0.1 M potassium phosphate buffer solution (pH 7.0) containing 0.1 mol L^{-1} KCl and 0.8 % Triton X-100 (V/V). The modified electrodes Fe_3O_4@C@Ag/ITO and silica/Fe_3O_4@C@Ag/ITO display no obvious redox peaks. When ChOx, ChEt and HRP were immobilized by silica/Fe_3O_4@C@Ag nanocomposite on the ITO electrode surface, one pair of well-shaped voltammetric peaks was observed.

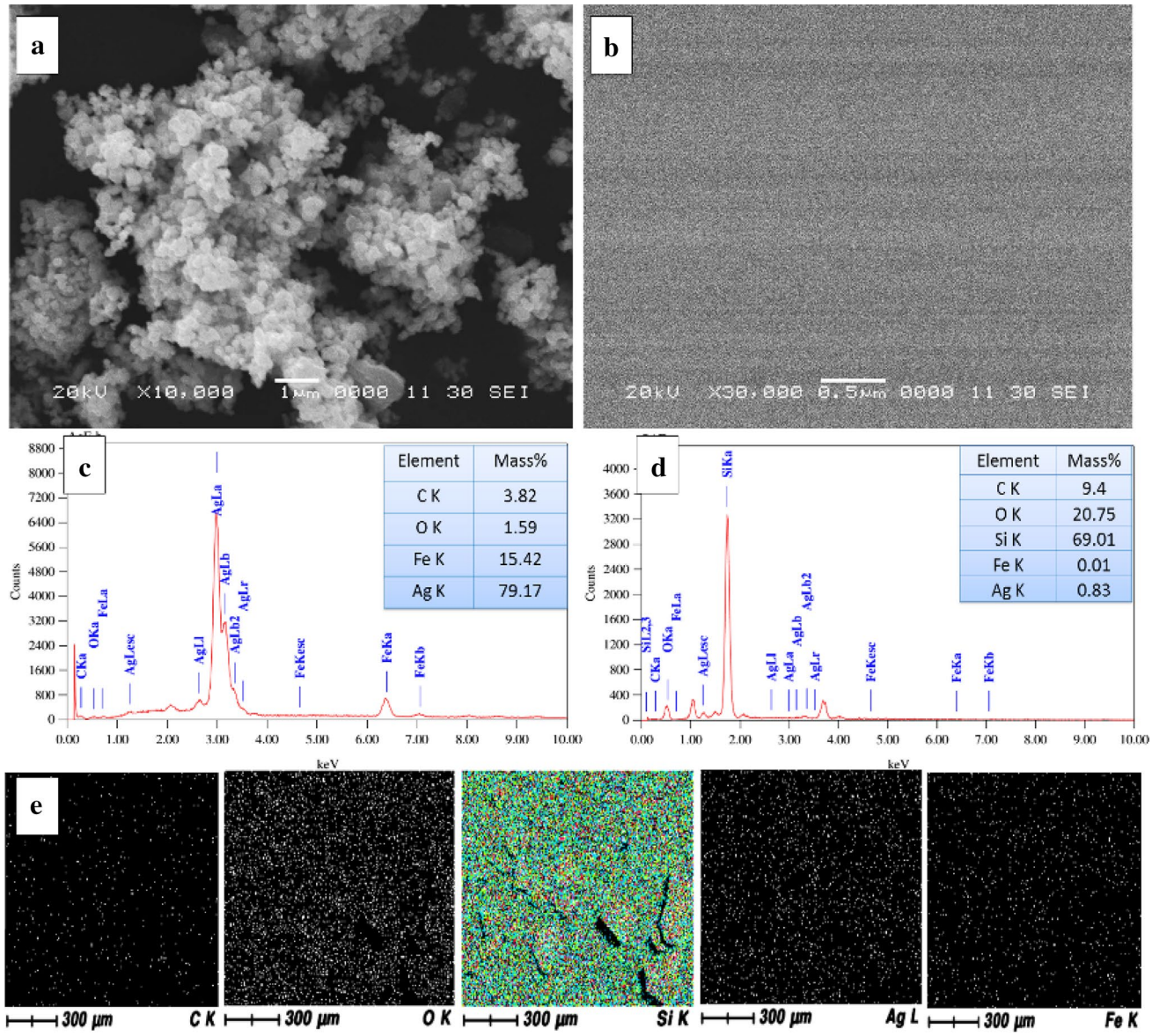

Fig. 4 SEM micrographs of **a** Fe_3O_4@C@Ag NPs, **b** Silica/Fe_3O_4@C@Ag nanocomposite; EDAX spectra with quantitative elemental composition of **c** Fe_3O_4@C@Ag NPs, **d** Silica/Fe_3O_4@C@Ag nanocomposite; and X-ray mapping analysis of **e** Silica/Fe_3O_4@C@Ag nanocomposite

Especially, a redox couple is significantly found at about $E^{0\prime} = 0.4$V ChOx (c), because the ChOx enzyme is a member of large family Flavin-specific oxidoreductases and exists in two different forms: (i) Flavin adenine dinucleotide (FAD) cofactor is covalently linked to the enzyme and (ii) FAD cofactor is non-covalently bound to the enzyme. Hither, the redox process is involving the $FAD/FADH_2$ redox couple of ChOx. The ChOx/ChEt/HRP/Silica/Fe_3O_4@C@Ag/ITO shows an obvious redox couple ($E^{0\prime} = 0.4$V) which is involving the $FAD/FADH_2$ redox process of ChOx. Further, it has been observed that the presence of Fe3O4@C@Ag NPs increases the overall background current.

3.7 Electrocatalytic Reaction of Cholesterol by ChOx/ChEt/HRP/Silica/Fe_3O_4@C@Ag/ITO

The electrocatalytic reaction of cholesterol (Fig. 8) was studied at ChOx/ChEt/HRP/Silica/Fe_3O_4@C@Ag/ITO modified electrode and the scan rate of 0.1 V s^{-1} in 0.1 M potassium phosphate buffer (pH 7.0). When cholesterol oleate was added, an obvious increase of peak current was observed, accompanied by the decrease of the oxidation peak current. The increment

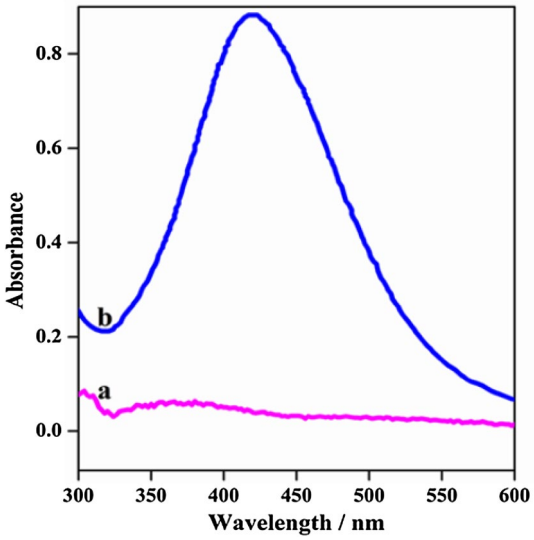

Fig. 5 UV–Visible spectra for **a** Fe_3O_4 NPs, and **b** Fe_3O_4@C@Ag NPs

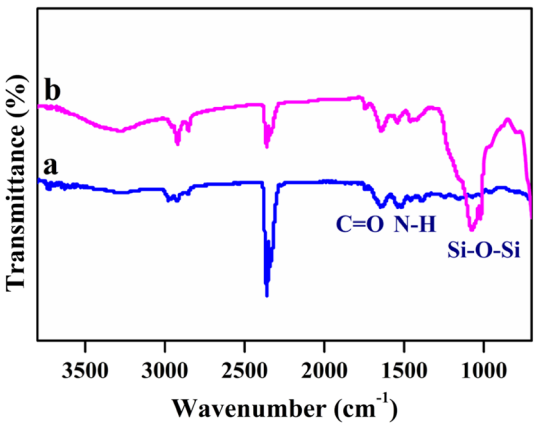

Fig. 6 FTIR spectra of **a** pure enzyme solution, and **b** Silica/Fe_3O_4@C@Ag/ChOx/ChEt/HRP

of reduction peak current became larger with the increasing cholesterol oleate concentration. It indicates that ChOx/ChEt/HRP/Silica/Fe_3O_4@C@Ag/ITO modified electrode exhibited excellent catalytic activity towards cholesterol oleate. The catalytic reduction peak current increased with the linear calibration equation $y = 0.0346x + 0.5201$ [mM] ($R^2 = 0.9955$) in the range from 0.5 to 22.5 mM of cholesterol oleate as shown in Fig. 8b. The sensitivity of modified electrode is 0.0346 µA mM^{-1} cm^{-1} with detection limit 0.5 mM.

This cathodic current response occurs due to the well-known reaction mechanism of cholesterol oxidation and the determination of H_2O_2. The enzymatic reaction with use of ChOx and ChEt can be described as follows equations [22]:

$$\text{Cholesterol} + O_2 \overset{ChOx}{\Rightarrow} \text{Cholest} - 4 - \text{en} - 3 - \text{one} + H_2O_2 \quad (1)$$

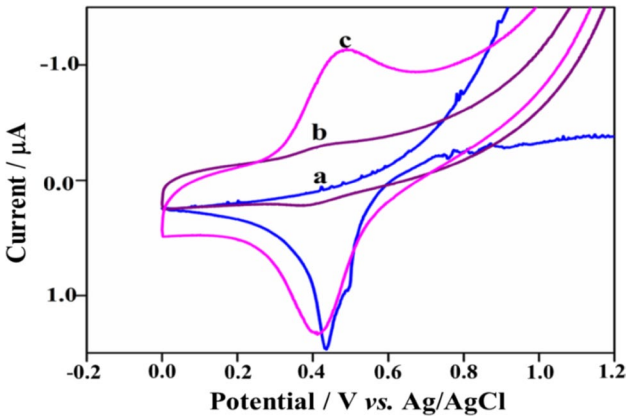

Fig. 7 Cyclic voltammograms of modified electrodes. **a** Fe_3O_4@C@Ag/ITO, **b** Silica/Fe_3O_4@C@Ag/ITO and **c** ChOx/ChEt/HRP/Silica/Fe_3O_4@C@Ag/ITO

$$\text{Cholesterol ester} + H_2O \overset{ChEt}{\Rightarrow} \text{Cholesterol} + \text{Fatty acids} \quad (2)$$

During the reductive half-reaction, the oxidized FAD cofactor accepts a hydride from the substrate and in the subsequent oxidative half-reaction, the reduced Flavin transfers the redox equivalents to molecular oxygen yielding hydrogen peroxide. ChEt enzyme catalyzes the hydrolysis of esterified cholesterol, thus allowing us to determine the total cholesterol. Since the H_2O_2 is the byproduct of cholesterol oxidation, the electro-reduction current of H_2O_2 can be further detected by ChOx/ChEt/HRP/Silica/Fe_3O_4@C@Ag/ITO modified electrode. The catalytic current response is directly proportional to cholesterol concentration. As the outcome, this electrode is found stable and electroactive for the electrocatalytic reduction of cholesterol.

3.7.1 Interferences Study

The influence of interfering substances on the response of cholesterol nanobiosensor was investigated. In particular, ascorbic acid and uric acid were focused, since these compounds are easily oxidized at the electrodes. It was found that four interfering substances uric acid, sucrose, glucose and ascorbic acid have no influence on the current response to cholesterol. It was also found that 10-fold concentration of ascorbic acid and uric acid cannot interfere with the detection of cholesterol at ChOx/ChEt/HRP/Silica/Fe3O4@C@Ag/ITO modified electrode. It suggests that nanobiosensor possesses high selectivity for the detection of cholesterol.

3.7.2 Real Sample Analysis

The application of the proposed method in real samples is investigated by the analysis of cholesterol in blood serum

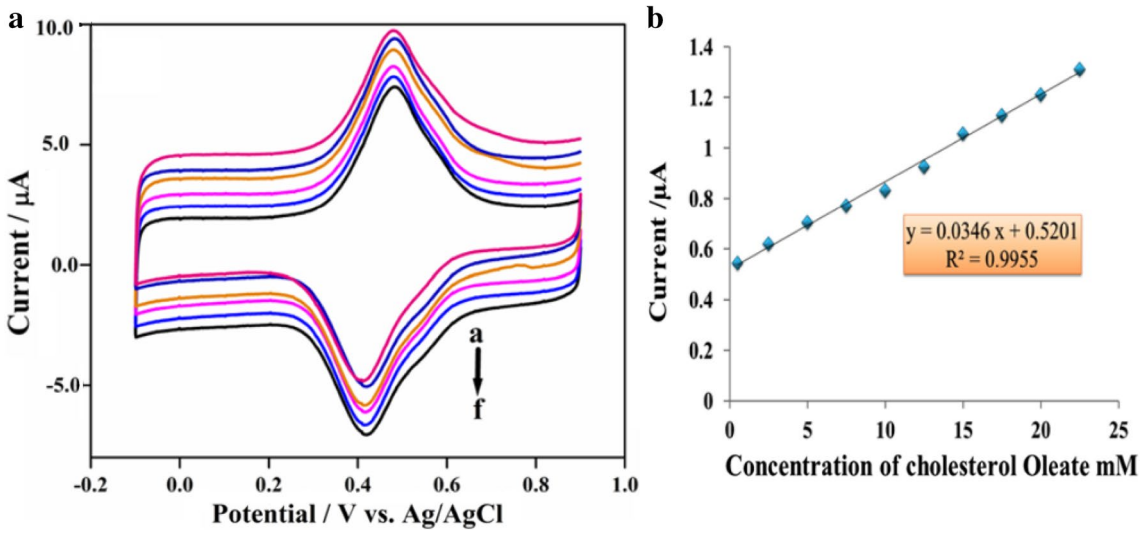

Fig. 8 Cyclic voltammograms of **a** ChOx/ChEt/HRP/Silica/Fe_3O_4@C@Ag/ITOmodified electrode in potassium phosphate buffer of pH 7.0 containing different concentration of cholesterol oleate from a to f at 0.1 V s^{-1} and **b** Plot of catalytic peak current versus cholesterol oleate concentration

Table 1 Determination of cholesterol oleate in blood serum sample

Sr. no.	Real sample	Added mM	Founded mM	Recovery %
1	Blood serum	0.0	–	–
2		5.0	5.25	105.0
3		10.0	10.10	101.0
4		15.0	14.72	98.1

using the standard addition method. It was carried out by using a different concentration of cholesterol oleate. The blood serum samples were collected from Dr. D.Y. Patil Hospital, Kolhapur and before use diluted 10-fold with potassium phosphate buffer (pH 7.0). The results are represented in Table 1 which shows, the obtained recoveries are in the range of 98–105%, suggesting that the proposed method have appropriate selectivity for cholesterol and can be successfully employed for the assay of cholesterol in real samples.

3.7.3 Stability and Reproducibility

The operational stability of the nanobiosensor has been assessed by consecutive measurements of a 5 mM cholesterol oleate sample. The relative standard deviation is 3.9 % for 10 measurements. For long term stability, theresponse of the nanobiosensor to 5 mM cholesterol oleate sample was monitored over a period of 6 weeks. The nanobiosensor shows 94 % of the initial response after 6 weeks. This slight decrease in response to cholesterol oleate of the nanobiosensor seems to be ascribed to the inactivation of the enzyme. In order to examine the reproducibility, the same nanobiosensor was used to measure the above cholesterol solution 70 times in 4 h, and the RSD was found to be 3.3 %.

4 Conclusion

A new silica nanocomposite has been successfully synthesized. Noteworthy, the method for the preparation of silica/Fe_3O_4@C@Ag nanocomposite is dealing with some promising potential applications in nano-biocatalysis and nano-bioelectronics. The high sensitivity of nanobiosensor is attributed to the large surface area of Fe_3O_4@C@Ag NPs for effective loading of enzymes as well its high electron communication capability with the aid of enhanced selectivity and anti-interference ability due to the silica sol–gel matrix. Nanobiosensor displays excellent selectivity, good reproducibility, and long-term stability. Furthermore, the electrode reveals both good operational and storage stability.

Acknowledgements Authors are very much grateful to D. Y. Patil University, Kolhapur for Financial support received under the D. Y. Patil University sponsored project DYPU/BMT/R&D/100.

References

1. Program, N. C. E. (1988). Report of the national cholesterol education program expert panel on detection, evaluation, and treatment of high blood cholesterol in adults. The expert panel. *Archives of Internal Medicine, 148,* 36–69.
2. Arya, S. K., Datta, M., & Malhotra, B. D. (2008). Recent advances in cholesterol nanobiosensor. *Nanobiosensors and Bioelectronics, 23*, 1083–1100.

3. Satvekar, R. K., Rohiwal, S. S., Raut, A. V., Karande, V. A., Tiwale, B. M., & Pawar, S. H. (2014). A silica-dextran composite as a novel matrix for immobilization of horseradish peroxidase, and its application to sensing hydrogen peroxide. *Microchimica Acta, 181*(1–2), 71–77.
4. Rohiwal, S. S., Satvekar, R. K., Tiwari, A. P., Raut, A. V., Kumbhar, S. G., & Pawar, S. H. (2015). Investigating the influence of effective parameters on molecular characteristics of bovine serum albumin nanoparticles. *Applied Surface Science, 334,* 157–164.
5. Tang, D., Yuan, R., & Chai, Y. (2006). Magnetic core-shell Fe_3O_4@Ag nanoparticles coated carbon paste interface for studies of carcinoembryonic antigen in clinical immunoassay. *Journal of Physical Chemistry B, 110*(24), 11640–11646.
6. Gee, S. H., Hong, Y. K., Erickson, D. W., Park, M. H., & Sur, J. C. (2003). Synthesis and aging effect of spherical magnetite (Fe_3O_4) nanoparticles for nanobiosensor applications. *Journal of Applied Physics, 93,* 7560.
7. Tiwari, A. P., Satvekar, R. K., Rohiwal, S. S., Karande, V. A., Raut, A. V., Patil, P. G., et al. (2015). Magneto-separation of genomic deoxyribosenucleic acid using pH responsive Fe3O4@silica@chitosan nanoparticles in biological samples. *RSC Advances, 5,* 8463.
8. Arica, M. Y., Yavuz, H., Patir, S., & Denizli, A. (2000). Epoxy-derived pHEMA membrane for use bioactive macromolecules immobilization: Covalently bound urease in a continuous model system. *Journal of Molecular Catalysis B*: *Enzymatic,* 11, 127.
9. Tong, X. D., Xue, B., & Sun, Y. (2001). A novel magnetic affinity support for protein adsorption and purification. *Biotechnology Progress, 17,* 134.
10. Rudge, S. R., Kurtz, T. L., Vessely, C. R., Catterall, L. G., & Williamson, D. L. (2000). Preparation, characterization, and performance of magnetic iron–carbon composite microparticles for chemotherapy. *Biomaterials, 21,* 1411.
11. Zhao, X., Xia, D., & Zheng, K. (2012). Fe_3O_4/Fe/carbon composite and its application as anode material for lithium-ion batteries. *ACS Applied Materials & Interfaces, 4,* 1350–1356.
12. Zhang, Z., Guo, C., Zhang, S., He, L., Wang, M., Peng, D., et al. (2016). Carbon-based nanocomposites with aptamer-templated silver nanoclusters for the highly sensitive and selective detection of platelet-derived growth factor. *Biosensors & Bioelectronics, 12*(89), 735–742.
13. Kawamoto, M., He, P., & Ito, Y., Green Processing of Carbon Nanomaterials. (2016). Green processing of carbon nanomaterials. *Advanced Materials*, 17.
14. Marquez, A. N., Romero, R., Romeroa, A., & Valverde, J. L. (2011). Carbon nanospheres: synthesis, physicochemical properties and applications. *Journal of Materials Chemistry, 21,* 1664.
15. Fan, W., Gao, W., Zhang, C., Weei, Tjiu W., Pan, J., & Liu, T. (2012). Hybridization of graphene sheets and carbon-coated Fe_3O_4 nanoparticles as a synergistic adsorbent of organic dyes. *Journal of Materials Chemistry, 22,* 25108.
16. Umar, A., Rahman, M. M., Al-Hajry, A., & Hahn, Y. B. (2009). Highly-sensitive cholesterol biosensor based on well-crystallized flower-shaped ZnO nanostructures. *Talanta, 7*(8), 284–289.
17. Fang, C., He, J., & Chen, Z. (2011). A disposable amperometric biosensor for determining total cholesterol in whole blood. *Sensors and Actuators B, 155,* 545–550.
18. Sekretaryova, A., Beni, V., Eriksson, M., Karyakin, A. A., Turner, A., & Vagin, M. (2014). Cholesterol self-powered biosensor. *Analytical Chemistry, 86*(19), 9540–9547.
19. Satvekar, R. K., Tiwari, A. P., Rohiwal, S. S., Tiwale, B. M., & Pawar, S. H. (2015). A DNA assembled Fe_3O_4@Ag nanorod in silica matrix for cholesterol biosensing. *Journal of Materials Engineering and Performance, 24*(12), 4691–4695.
20. Satvekar, R. K., Phadatare, M. R., Karande, V. A., Patil, R. N., Tiwale, B. M., & Pawar, S. H. (2012). Influence of silane content on the optical properties of sol gel derived spin coated silica thin films. *International Journal of Basic and Applied Sciences, 1,* 468–476.
21. Charpentier, L., & Murr, N. E. I. (1995). Amperometric determination of cholesterol in serum with use of a renewable surface peroxidase electrode. *Analytica Chimica Acta, 318,* 89.
22. Satvekar, R. K. (2015). Chapter 8, Thesis: Studies on development and performance of silica nanocomposite based enzyme nanobiosensors. http://hdl.handle.net/10603/51072